

Spin density-functional theory for imbalanced interacting Fermi gases in highly elongated harmonic traps

Gao Xianlong

Department of Physics, Zhejiang Normal University, Jinhua, Zhejiang Province, 321004, China

Reza Asgari

School of Physics, Institute for Studies in Theoretical Physics and Mathematics, 19395-5531 Tehran, Iran

(Dated: January 13, 2019)

We numerically study imbalanced two component Fermi gases with attractive interactions in highly elongated harmonic traps. An accurate parametrization formula for the ground state energy is presented for a spin-polarized attractive Gaudin-Yang model. Our studies are based on an accurate microscopic spin-density-functional theory through the Kohn-Sham scheme which employs the one-dimensional homogeneous Gaudin-Yang model with Luther-Emery-liquid ground-state correlation as a reference system. A Thomas-Fermi approximation is examined incorporating the exchange-correlation interaction. By studying the charge and spin density profiles of the system based on these methods, we gain a quantitative understanding of the role of attractive interactions and polarization on the formation of the two-shell structure, with the coexisted Fulde-Ferrell-Larkin-Ovchinnikov-type phase in the center of the trap and either the BCS superfluid phase or the normal phase at the edges of the trap. Our results are in good agreement with the recent theoretical consequences.

PACS numbers: 03.75.Ss,71.15.Mb,71.10.Pm

I. INTRODUCTION

Progress made in trapping ultracold atomic gases into different low-dimensional systems [1, 2] has provided us grounds to describe and simulate the behavior of fascinating non-Fermi liquid in which the analysis may not be as tractable. The physical properties of such systems have attracted both experimental and theoretical interest.

For the research in the experimental side, the Tonks-Girardeau regime of strongly repulsive bosons in one-dimensional (1D) systems has been observed [2]. This regime is understood through the mapping of the strongly repulsive, impenetrable bosons onto an ideal gas of fermions subjected to the same external potential [3]. Esslinger and colleagues at ETH Zurich in Switzerland confined a two-component Fermi gas of ^{40}K atoms to thousands of highly elongated one-dimensional tubes. Such a system is realized by using a two-dimensional optical lattice, having about 100 atoms in each tube [1] and serves as a 1D matter waveguide to observe the two-particle bound states of atoms. For the first time, they created confinement induced molecules. The binding energy of the molecules is measured by using radio-frequency spectroscopy bearing a good agreement with the theoretical predictions [4]. Importantly, two-particle bound molecular states are formed in 1D confined system independent of the nature of the interaction, i.e., attrac-

tive or repulsive between atoms. This is obviously different from what happens in free space where a molecule is formed only when the atoms attract.

On the other hand, many theoretical efforts on quasi-one dimensional (Q1D) inhomogeneous Fermi gases have been made. For 1D trapped fermions at finite temperature with attractive binary interactions, the transition to a fermion-paired state is obtained by exact stochastic mean-field calculations [5], which is characterized by dominant Cooper pairing correlations, an algebraic long-range order and a superfluid component. A one-dimensional spin-polarized Fermi gas with infinitely strong attractive zero-range odd-wave interactions has been studied. This system is known as the fermionic Tonks-Girardeau gas, arising from a confinement-induced resonance reachable via a three-dimensional p-wave Feshbach resonance [6]. In Ref. [7], a bosonization technique has been developed to calculate analytically the density profile, the momentum distribution, and several correlation functions of two-component Fermi gases with inclusion of forward-scattering processes and exclusion of backward scattering between inter-components. Inhomogeneous Tomonaga-Luttinger liquid model, with space-dependent parameters assuming a slowly varying trap potential on the scale of the Fermi wavelength, has been used to describe spin-charge separation in two-component Fermi gases [8, 9]. The Thomas-Fermi approximation is widely used to calculate the ground state

properties of a large system [9, 10]. The existence of a molecular Tonks-Girardeau gas is predicted for strong attractive effective interactions [10]. In Ref. [11] a microscopic calculation of the density-functional theory (DFT), based on the exact Bethe-ansatz solution of 1D homogeneous Gaudin-Yang system, is presented for the ground-state density profile with arbitrary size. Quantitative understanding about the role of the repulsive or attractive interactions on the shell structure of the axial density profile is achieved.

Above mentioned studies are focused on the fully polarized Fermi atomic gases. Recently, progress in two experiments [12, 13] in trapping partially polarized Fermi atomic gases has paved the way for systematic studies on systems with different number of spin-up and spin-down atoms ($N_\uparrow \neq N_\downarrow$). The experiment explored on three-dimensional polarized ${}^6\text{Li}$ gases [12] suggested that the density profiles show coexisting three-shell structures: a fully unpolarized paired superfluid phase in the center of the trap, a fully polarized noninteracting phase composed of excess atoms, and a partially polarized normal shell between these two regions. The experiment which employed an elongated cigar-shaped trap of polarized ${}^6\text{Li}$ gases [13] suggests the gas separates into a phase that is consistent with a superfluid paired core surrounded by a shell of normal unpaired fermions beyond a critical polarization.

Recently two theoretical investigations [14, 15] discussed partially polarized two-component Fermi gases of attractive interaction within local density approximation while implementing the exact exchange-correlation interaction from the homogeneous Bethe-ansatz solution of 1D Gaudin-Yang model. Both of these two papers predict a two-shell density profile structure of a coexisting partially polarized superfluid core in the center of the trap while at the edges of the trap either fully paired or fully polarized wings depending on the attractive interaction strength and the polarization. Furthermore, they anticipated a critical spin polarization and a non-monotonic behavior of the Thomas-Fermi radius of each spin component as a function of the polarization. Orso [14] and Hu et al. [15] identified the polarized superfluid as having the Fulde-Ferrell-Larkin-Ovchinnikov (FFLO) structure, which is stabilized in a polarized two-component Fermi gas in an array of weakly-coupled 1D tubes [16]. These two theoretical efforts used the local-density approximation for the harmonic trap and Thomas-Fermi-

type approximation for the interaction. The local-density approximation is applicable when $N \gg 1$, where N is the number of particles, but deteriorates with decreasing particle number and completely neglects the tunneling of the density profile beyond the Thomas-Fermi radius where one instead needs to use a method beyond the local-density approximation, like the microscopic density-functional theory.

The FFLO phenomena of imbalanced fermion populations in 1D optical lattices of attractive interactions have also been extensively discussed recently [17, 18, 19], where FFLO pairing is formed robust from the attractive interaction for a wide range of polarization, and for the spatial inhomogeneities induced by the presence of a trap in the experimental reality.

In this paper, we study 1D harmonically trapped Fermi gases of imbalanced spin population with two alternative approaches. One is the spin-density-functional theory based on the Bethe-ansatz results for the 1D Luttinger liquid, which is specially useful for systems whose analytical solutions or exact numerical methods are not available, and the other is the Thomas-Fermi approximation based on the non-interacting approximation for the kinetic energy. Both methods consider exactly the exchange-correlation energy of the corresponding 1D homogeneous system. Within these two methods, we quantitatively study the systems of weak and intermediate coupling strength and different polarizations by analyzing the charge and spin density profiles.

The paper is organized as follows. In Sec. II we introduce our model and present the parametrization result for the ground state energy of the homogeneous Gaudin-Yang model. In Sec. III the spin-density-functional theory is briefly discussed. Numerical results and discussion are presented in Sec. IV. Finally, we conclude in Sec. V.

II. THE MODEL AND ITS PARAMETRIZATION RESULT

A system of N spin-1/2 fermions is considered to be one-dimensional when subjected to a strongly anisotropic harmonic potential with angular frequencies in the radial direction ω_\perp much larger than that in the axial direction ω_\parallel with $\omega_\parallel/\omega_\perp \ll N^{-1}$. We consider two kind of fermion particles with mass m , interacting *via* a δ -type contact with an effective 1D coupling strength g_{1D} in the harmonic trap. The Hamiltonian for such a system is given

by

$$\mathcal{H} = -\frac{\hbar^2}{2m} \sum_{i=1}^N \frac{\partial^2}{\partial z_i^2} + g_{1D} \sum_{i=1}^{N_\uparrow} \sum_{j=1}^{N_\downarrow} \delta(z_i - z_j) + \frac{1}{2} m \omega_{\parallel}^2 \sum_{i=1}^N z_i^2. \quad (1)$$

Note that when p-wave interactions are neglected, the contact s-wave interactions between same species are suppressed by the Pauli exclusion principle. The coupling constant g_{1D} can be written in terms of the scattering strength as $g_{1D} = -2\hbar^2/(a_{1D}m)$. The effective 1D scattering length a_{1D} can be expressed through the three-dimensional scattering length a_{3D} for fermions confined in a quasi-1D geometry, $a_{1D} = -a_{\perp}^2(1 - Aa_{3D}/a_{\parallel})/a_{3D} > 0$ with the constant $A \approx 1.0326$ [4]. In the following, we will choose the harmonic-oscillator length $a_{\parallel} = \sqrt{\hbar/(m\omega_{\parallel})}$ as unit of length and the harmonic-oscillator quantum $\hbar\omega_{\parallel}$ as unit of energy.

Without the external potential the Hamiltonian (1) reduces to the homogeneous Gaudin-Yang model, which is exactly solvable by use of the Bethe-ansatz method [20]. In the thermodynamic limit, the system is determined by the spin polarization $\zeta = (N_{\uparrow} - N_{\downarrow})/N$ and a dimensionless parameter $\gamma \equiv mg_{1D}/(\hbar^2n)$, while in the fully unpolarized system the only parameter of the system is γ . We denote the charge density as $n = N/L$ and the spin density $s = (N_{\uparrow} - N_{\downarrow})/2L = (n_{\uparrow} - n_{\downarrow})/2$.

For N attractive fermions, the ground state is described by the coupled integral equations for the momentum distribution $\rho(k)$ and $\sigma(\lambda)$,

$$\rho(k) = \frac{1}{2\pi} + \frac{2\gamma n}{\pi} \int_{-B}^B d\lambda \frac{1}{(\gamma n)^2 + 4(k - \lambda)^2} \sigma(\lambda), \quad (2)$$

and

$$\sigma(\lambda) = \frac{1}{\pi} + \frac{2\gamma n}{\pi} \int_{-Q}^Q dk \frac{1}{(\gamma n)^2 + 4(k - \lambda)^2} \rho(k) + \frac{\gamma n}{\pi} \int_{-B}^B d\lambda' \frac{1}{(\gamma n)^2 + (\lambda - \lambda')^2} \sigma(\lambda'), \quad (3)$$

where B and Q are non-negative numbers related to the normalization conditions

$$\int_{-Q}^Q dk \rho(k) = 2s \quad (4)$$

and

$$\int_{-B}^B d\lambda \sigma(\lambda) = \frac{n}{2} - s. \quad (5)$$

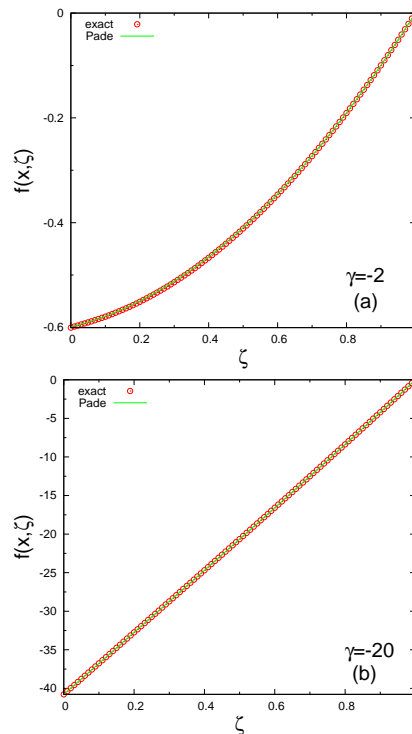


FIG. 1: (color online) The interaction contribution $f(\zeta, x) = [\varepsilon_{\text{GS}}(n, \zeta, \gamma) - \kappa(n, \zeta)]/E_{\text{F}}$ to the ground state energy of the homogeneous Gaudin-Yang model as a function of the spin polarization ζ for (a) $\gamma = -2$ and (b) $\gamma = -20$. The exact result, obtained from the solution of the Bethe-Ansatz Eqs. (2)-(5), is compared with the parametrization formula given by Eq. (7).

The ground state energy (GSE) per particle is written in terms of the momentum distributions $\rho(k)$ and $\sigma(\lambda)$ as

$$\frac{E}{N} = \frac{1}{n} \frac{\hbar^2}{2m} \left[\int_{-Q}^Q dk k^2 \rho(k) + 2 \int_{-B}^B d\lambda [\lambda^2 - (\gamma n/2)^2] \sigma(\lambda) \right]. \quad (6)$$

For N repulsive fermions interacting *via* a δ -type contact, the correlation energy per particle, and then the GSE, has been parameterized based on Padé approximant in [21, 22, 23]. Magyar achieved an improved parametrization results for the correlation energy by including the higher-order correlation kernel terms at the high-density limits which is needed for the adiabatic time-dependent DFT approximation [23].

For the present system of attractive contact interacting, we solve numerically a set of coupled Eqs.(2)-(5) and find the GSE per particle $\varepsilon_{\text{GS}}(n, \zeta, \gamma) \equiv E/N$ given in Eq. (6) as a function of n , ζ and γ . After having

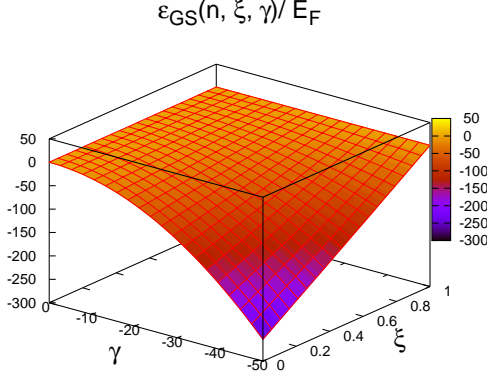


FIG. 2: (color online) The ground state energy per particle in unit of Fermi energy as functions of ζ and γ .

$\varepsilon_{\text{GS}}(n, \zeta, \gamma)$, we find an accurate parametrization formula to fit $\varepsilon_{\text{GS}}(n, \zeta, \gamma)$. Our parametrization formula is

$$\varepsilon_{\text{GS}}(n, \zeta, \gamma) = \kappa(n, \zeta) + f(\zeta, x)E_{\text{F}}, \quad (7)$$

where

$$\kappa(n, \zeta) = \frac{\pi^2 \hbar^2 n^2}{24m} (1 + 3\zeta^2) \quad (8)$$

is the kinetic energy of the noninteracting system per particle and the Fermi energy is $E_{\text{F}} = \hbar^2 n^2 \pi^2 / (8m)$. Here, $f(\zeta, x)$ can be represented by,

$$f(\zeta, x) = [e(x) - 1/3] \{1 + \alpha(x)|\zeta| + \beta(x)\zeta^2 - [1 + \alpha(x) + \beta(x)]|\zeta|^3\}, \quad (9)$$

where $x = 2\gamma/\pi$, $e(x)$ is given in Ref. [11] very accurately as,

$$e(x) = \frac{1}{3} - \frac{|x|}{\pi} - \frac{x^2 + a_m|x| + b_m x^2}{x^2 + c_m|x| + d_m} \frac{1}{4} \quad (10)$$

with $a_m = -0.331117$, $b_m = 0.458183$, $c_m = a_m + 4/\pi$, and $d_m = 4a_m/\pi + b_m + 16/\pi^2 - 1$. Equation (10) gives the exact asymptotic behaviors at $x \rightarrow 0^-$ and $x \rightarrow -\infty$ [10]. $\alpha(x)$ and $\beta(x)$ are given by Padé approximant,

$$\begin{cases} \alpha(x) = \frac{x^3 + A_\alpha x}{-x^3 + B_\alpha x + C_\alpha} \\ \beta(x) = \frac{A_\beta x + B_\beta}{x^3 + C_\beta x^2 + D_\beta x - B_\beta} \end{cases}. \quad (11)$$

Here $A_\alpha = -0.0652385$, $B_\alpha = -1.87353$, $C_\alpha = 3.08873$, $A_\beta = 3.90515$, $B_\beta = 19.4239$, $C_\beta = -4.53457$ and $D_\beta = -7.29826$.

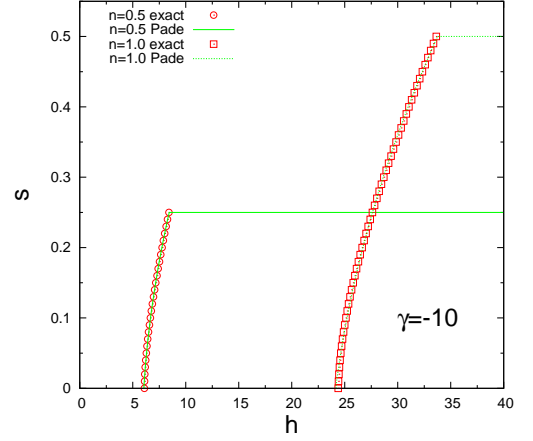


FIG. 3: (color online) The magnetization (in units of the inverse of arbitrary length a) as a function of magnetic field (in units of \hbar^2/ma^2) for different fillings at $n = 0.5$ and $n = 1.0$ for given $\gamma = -10$ (n is taken also in units of the inverse of arbitrary length a , in the text we take the same units as described here.). The exact results from Bethe-Ansatz equations are compared with those derived from the parametrization formula.

To assess the validity of our parameterized formula, we show in Fig. 1 the results emerging from Eq. (7) in comparison with the exact Bethe-Ansatz results for $\gamma = -2$ and $\gamma = -20$ in the weak and strong attractive regime, respectively. As it is clear from Fig. 1, our parametrization formula has an excellent agreement with the exact calculation and it would be safe to use the parametrization formula for all range of n , ζ and γ values.

Here we would like to deal with some asymptotic behaviors of the simple parametrization formula in Eq. (7). First of all, we can simply obtain both unpolarized ($\zeta = 0$) and polarized ($\zeta = 1$) limits exactly. Secondly, the weak interacting regime [24] is recovered after taking $\gamma \rightarrow 0$ limit in Eq. (7) as

$$\varepsilon_{\text{GS}}(n, \zeta, \gamma \rightarrow 0) = \frac{\hbar^2 \pi^2 n^2}{24m} (1 + 3\zeta^2) + \frac{\hbar^2 n^2}{4m} (1 - \zeta^2) \gamma + O(\gamma^2).$$

The strongly attractive limit from our parametrization formula is

$$\varepsilon_{\text{GS}}(n, \zeta, \gamma \rightarrow -\infty) = -\frac{\hbar^2 n^2}{8m} (1 - \zeta) \gamma^2 + \frac{\hbar^2 \pi^2 n^2}{96m} (1 + 15\zeta) + O\left(\frac{1}{\gamma}\right)$$

which has little difference comparing with Batchelor's

derivation [24]

$$\begin{aligned} \varepsilon_{\text{GS}}(n, \zeta, \gamma \rightarrow -\infty) &= -\frac{\hbar^2 n^2}{8m}(1 - \zeta)\gamma^2 + \frac{\hbar^2 \pi^2 n^2}{96m} \\ &\times (1 + 15\zeta^3 - 3\zeta + 3\zeta^2) + O\left(\frac{1}{\gamma}\right). \end{aligned}$$

For emphasizing these limits, we show $\varepsilon_{\text{GS}}(n, \zeta, \gamma)/E_F$ as functions of ζ and γ in Fig. 2. At $\zeta = 0$, $\varepsilon_{\text{GS}}(n, 0, \gamma)/E_F$ behaves like $-\gamma$ at weak attractive limit and $-\gamma^2$ at strong attractive one, while at $\zeta = 1$, $\varepsilon_{\text{GS}}(n, 1, \gamma)/E_F$ goes as a constant. The expression at strong interaction limit differs from the corresponding repulsive case due to the attractive nature of the interaction. Furthermore $\varepsilon_{\text{GS}}(n, \zeta, \gamma)/E_F$ behaves like ζ^2 at weak attractive limit similar to the corresponding repulsive 1D expression, however it behaves like ζ at strong attractive limit.

Furthermore, we would like to examine some other physical quantities calculated from Eq. (7) in comparison to those calculated within the exact Bethe-Ansatz equations to obtain more credibility for our parametrization formula. For this purpose, we take the derivative of the ground state energy with respect to the magnetization to calculate the magnetic field in equilibrium condition which is $h(n, s, \gamma) = \partial[n\varepsilon_{\text{GS}}(n, \zeta, \gamma)]/\partial s$ [25]. The magnetization vanishes when the field becomes smaller than the critical value h_c , a term associated with the spin energy gap in the attractive case (Note that it vanishes in the repulsive case.). We next display the exact magnetization as a function of the magnetic field solved numerically from the coupled integro-differential equations based on Eqs. (2)-(5) in comparison to those derived from the parametrization formula.

For given $\gamma = -10$, the exact numerical calculation gives $h_c = 6.097$ for $n = 0.5$, while from the parametrization formula we get $h_c = 6.049$ for the same density as shown in Fig. 3. Moreover, $h_c = 24.388$ for $n = 1.0$, by calculating exact formula and we have $h_c = 24.182$ from parametrization formula. Surprisingly, a finite magnetization appears only if the magnetic field larger than h_c . The magnetization saturates at $s = n/2$ when $h > h_s$. More precisely, for $\gamma = -10$, the exact solution of h_s is 8.410 for $n = 0.5$, and 33.643 for $n = 1.0$, which are very close to values obtained from the parametrization formula that we get $h_s = 8.440$ and 33.759, respectively.

After comparing the exact solutions to the parametrization formula, we convince that the parametrization formula gives satisfying simulations on

the ground state energy and the derivative quantities like the chemical potential and the magnetic field in a wide range of parameters.

III. SPIN-DENSITY-FUNCTIONAL THEORY AND THOMAS-FERMI APPROXIMATION

The ground-state spin densities $n_\sigma(z)$ can be calculated by spin-density-functional theory (SDFT) solving self-consistently the Kohn-Sham equations

$$\left[-\frac{\hbar^2}{2m} \frac{\partial^2}{\partial z^2} + V_{\text{KS}}^{(\sigma)}[n_\sigma](z) \right] \varphi_{\alpha, \sigma}(z) = \varepsilon_{\alpha, \sigma} \varphi_{\alpha, \sigma}(z) \quad (12)$$

with effective potential $V_{\text{KS}}^{(\sigma)}[n_\sigma](z) = V_{\text{H}}^{(\sigma)}[n_\sigma](z) + V_{\text{xc}}^{(\sigma)}[n_\sigma](z) + m\omega_{\parallel}^2 z^2/2$. The ground state density is determined by the closure

$$n_\sigma(z) = \sum_{\alpha=1}^{\text{occ.}} \Gamma_{\alpha}^{(\sigma)} |\varphi_{\alpha, \sigma}(z)|^2. \quad (13)$$

Here the sum runs over the occupied orbitals and the degeneracy factors $\Gamma_{\alpha}^{(\sigma)}$ satisfy the sum rule $\sum_{\alpha} \Gamma_{\alpha}^{(\sigma)} = N_{\sigma}$. The spin-dependent effective Kohn-Sham (KS) potential as usual is composed by the mean-field term $V_{\text{H}}^{(\sigma)} = g_{1\text{D}} n_{\sigma}(z)$, the exchange-correlation potential defined as the functional derivative of the exchange-correlation energy $E_{\text{xc}}[n_{\sigma}]$ evaluated at the ground-state density profile, $V_{\text{xc}}^{(\sigma)} = \delta E_{\text{xc}}[n_{\sigma}]/\delta n_{\sigma}(z)|_{\text{GS}}$, and the external potential, respectively.

In order to calculate $n_{\sigma}(z)$, E_{xc} needs to be approximated. Here we take the local-spin-density approximation (LSDA) which is known to provide an excellent description of the ground-state properties of a variety of inhomogeneous systems [26] to calculate. In the following we employ an LSDA functional based on the parametrization results of Eq. (7) for the exchange-correlation potential,

$$E_{\text{xc}}[n_{\sigma}] = \int dz n(z) \varepsilon_{\text{xc}}^{\text{hom}}(n, \zeta, \gamma) \Big|_{n \rightarrow n(z), \zeta \rightarrow \zeta(z)}. \quad (14)$$

The exchange-correlation energy $\varepsilon_{\text{xc}}^{\text{hom}}$ of the homogeneous Gaudin-Yang model is defined as

$$\varepsilon_{\text{xc}}^{\text{hom}}(n, \zeta, \gamma) = \varepsilon_{\text{GS}}(n, \zeta, \gamma) - \kappa(n, \zeta) - \varepsilon_{\text{H}}(n, \zeta, \gamma).$$

Here $\varepsilon_{\text{H}}(n, \zeta, \gamma) = \frac{\hbar^2 n^2}{4m} \gamma(1 - \zeta^2)$ comes from the contribution of the Hartree-Fock mean field.

Following the above points, we write down conveniently the Kohn-Sham potential as,

$$V_{\text{KS}}^{(\sigma)}[n_\sigma](z) = \frac{1}{2}m\omega_{\parallel}^2 z^2 + \mu[n, s](z) - \mu_0[n, s](z) \pm \frac{1}{2} \{h[n, s](z) - h_0[n, s](z)\}, \quad (15)$$

where $\mu[n, s](z) = \partial[n\varepsilon_{\text{GS}}(n, \zeta, \gamma)]/\partial n|_{n \rightarrow n(z), s \rightarrow s(z)}$ is the chemical potential and $h[n, s](z) = \partial[n\varepsilon_{\text{GS}}(n, \zeta, \gamma)]/\partial s|_{n \rightarrow n(z), s \rightarrow s(z)}$ the magnetic field of the homogeneous system evaluated at the local potentials, respectively. $\mu_0[n, s](z)$ and $h_0[n, s](z)$ are the corresponding chemical potential and magnetic field of the noninteracting system, which are given by

$$\mu_0[n, s](z) = \frac{\hbar^2 \pi^2}{8m} [n^2(z) + 4s^2(z)],$$

$$h_0[n, s](z) = \frac{\hbar^2 \pi^2}{m} n(z)s(z).$$

Here, $n(z) = n_{\uparrow}(z) + n_{\downarrow}(z)$ is the total density distribution, and $s(z) = [n_{\uparrow}(z) - n_{\downarrow}(z)]/2$ is the spin density distribution or the local magnetization.

From the discussions in Sec. (II), we know that our spin-density-functional theory with the reference system based on Bethe-ansatz equations has correctly incorporated the Luther-Emery-liquid nature and the spin energy gap of the homogeneous system [27, 28]. The inhomogeneity nature induced by the harmonic trap will be incorporated into the exchange-correlation potential through the local spin-density approximation. Hereafter we refer to this method as BALSDA.

Another simplified method to describe this inhomogeneous system is to resort to a local density approximation (LDA) also for the noninteracting kinetic energy function, which is a Thomas-Fermi approximation (TFA) similar to the TFA but implementing the exchange-correlation energy. We refer to this approach as the TFA in the following. Within the LDA one assumes that the chemical potential of the trapped system is given by the sum of the spin-dependent local chemical potential taken to be the chemical potential of the uniform system at the corresponding density, and the external potential. The ground-state density profile is obtained in the spirit of the local equilibrium condition,

$$\mu_{\sigma}^0 = \mu_{\sigma}^{\text{hom}}[n_{\uparrow}, n_{\downarrow}](z) + m\omega_{\parallel}^2 z^2/2 \quad (16)$$

derived by directly minimizing the total energy functional of the system. The constants μ_{σ}^0 are fixed by the normalization condition $N_{\sigma} = \int dz n_{\sigma}(z)$, and $\mu_{\sigma}^{\text{hom}}[n_{\uparrow}, n_{\downarrow}](z)$,

the corresponding density dependent chemical potentials of the homogeneous system is derived from the parametrization formula in Eq. (7) evaluated at the local densities of $n_{\uparrow}(z)$ and $n_{\downarrow}(z)$. Within the LDA, a dimensionless characteristic parameter $\eta = Na_{1D}^2/a_{\parallel}^2$ can be defined in the harmonic trap. The systems hold the same density profile if the characteristic parameter is the same irrespective of their different number of particles and different harmonic oscillators [10]. The parameter can be also expressed as, $\eta = 4N/\Lambda^2$ with $\Lambda = g_{1D}/(a_{\parallel}\hbar\omega_{\parallel})$ if we keep in mind that $\gamma = -2/(na_{1D})$. $\eta \gg 1$ corresponds to weak coupling while $\eta \ll 1$ corresponds to the strong interacting regime.

IV. NUMERICAL RESULTS

In this section we present the numerical results obtained from the self-consistent solution of Eqs. (12)-(15) using our accurate parametrization formula from Padé approximant. We test the TFA approach and compare its results with our full BALSDA to justify how advance physics we have within BALSDA. We proceed to illustrate our main numerical results, which are summarized in Figs. 4-5.

First of all, we show the ground state site occupation for a Fermi gas trapped in a harmonic potential at different polarizations in Fig. 4. Here $\Lambda = -2$ which implies $\eta = N$, corresponding to weak coupling regime. For the harmonically confined system, we define the average polarization as $P = (N_{\uparrow} - N_{\downarrow})/(N_{\uparrow} + N_{\downarrow})$, which is changed keeping always a constant number of spin-up atoms N_{\uparrow} and decreasing N_{\downarrow} . $P = 0$ means an unpolarized system and $P = 100\%$ corresponds to a trivial fully polarized case of N_{\uparrow} noninteracting fermions. The density profiles of spin-up and spin-down atoms show N_{\uparrow} and N_{\downarrow} maxima, respectively [11], which reflects in the total density profile with N_{\downarrow} maxima and in the spin one with N_{\downarrow} minimum.

In Fig. 4(a), the total charge density profile is shown as a function of z . The 'hat'-structure is formed in the bulk region by paired minority species of spin-down and spin-up atoms, manifested by N_{\downarrow} peaks inside and partially polarized fermions. Higher polarization gives smaller 'hat'-structure. By increasing the polarization P but keeping N_{\uparrow} constant, the range of the charge density becomes a little larger because the attractive interaction becomes weaker due to the decreasing spin down atoms.

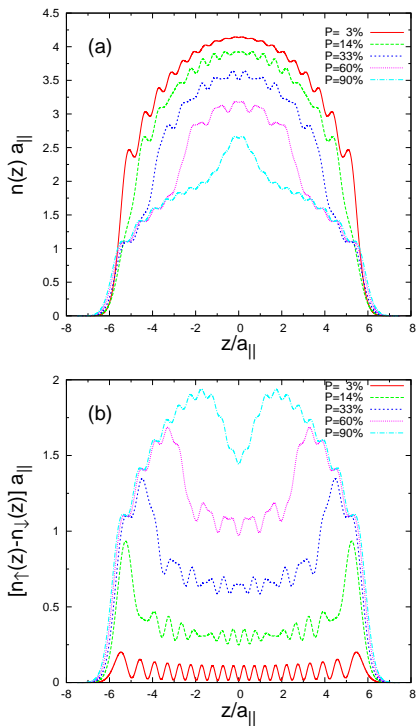


FIG. 4: (color online) The charge density (a) and spin density (b) profiles as a function of z for different polarization P at $\Lambda = -2$. The polarization is increased from 3% to 90% by keeping always a constant number of spin-up atoms, $N_{\uparrow} = 20$ and decreasing N_{\downarrow} from 19 to 1.

Orso [14] and Liu et al. [15, 29], after analyzing the phase diagram and calculating the order parameter, concluded that the state at the center of trap gives a two-shell structure of the FFLO-type, which has a spatially oscillatory behavior in the superconducting correlation function and exists in any nonzero polarization and attractive interaction. In Fig. 4(b), we show the spin density profile defined as the difference between spin-up and spin-down density, namely the local magnetization as a function of z . By increasing the P value, an oscillating structure of the spin density wave appears in the bulk of the system, due to the attractive interaction between the majority and minority species. As a result, a quasi-flat region appears in the bulk part of the spin density profile with coexisted spin-up and spin-down atoms, surrounded by fully polarized spin-up atoms only. The core of coexisting spin-up and spin-down atoms becomes smaller and smaller for higher value of P . We would like to point out that the local magnetization distribution as a function of position is directly measurable through phase-contrast imaging techniques [30].

In Fig. 5, we show the spin-up, spin-down density profiles, and furthermore, the local magnetization distribution at $\Lambda = -12$ with fixed total atom number of $N = 36$ but varying spin-up and spin-down atoms. This implies $\eta = 1$, corresponding to an intermediate coupling regime. From Figs. 5(a), (b) and (c), it is clear that the amplitude of the oscillations increases with decreasing P . We present results obtained by the TFA approach together with BALSDA to justify quantum effects. The TFA results are shown by solid lines between the oscillating density profiles. For $P = 0.56$, see Fig. 5(a), the TFA results give a good representation of the actual density profile, except at the edges of the cloud. We stress here, without including the exchange-correlation effect, the TFA gives bad overall shape for the density profiles.

In Fig. 5(a), a high polarization case of $P = 0.56$ is presented for the spin-up density, spin-down density and the spin-density profiles. It is clear that the curve envelop produces an oscillating structure particularly in Figs. 5(b) and 5(c). A two-shell structure is formed with a partially polarized FFLO superfluid in the center of the trap [29] and a fully polarized normal state of excess spin-up atoms at the edges. In Fig. 5(b), a polarization case of $P = 0.11$ is illustrated with BALSDA together with TFA, where a different two-shell structure is formed with a partially polarized superfluid at the trap center and a fully paired BCS superfluid state at the edges, opposite to the 3D counterpart of the BCS paired phase in the core. In the present system, we observe that there is one critical point which is $P_c = 0.12$ between the two above-mentioned different phase separations which coincides with the calculations given by Refs. [14, 15]. We want to stress here, from Fig. 5(a) to Fig. 5(b), due to the stronger attractive interaction when the size of the cloud shrinks considerably by decreasing P , that the oscillation structure due to correlation effects become more important and the LDA result becomes worse. In Fig. 5(c), an even smaller polarization case of $P = 0.06$ is illustrated with BALSDA against TFA results. The fully paired superfluid state becomes larger in the wings with such a smaller polarization. The different phases in the two-shell structure of standard BCS state outside of the center and the FFLO-type state in the bulk, are proved to be a smooth second-order transformation [29]. In all the above calculations with weak and intermediate coupling regimes, we find the TFA results give a good overall shape to the microscopic calculations based on the BALSDA.

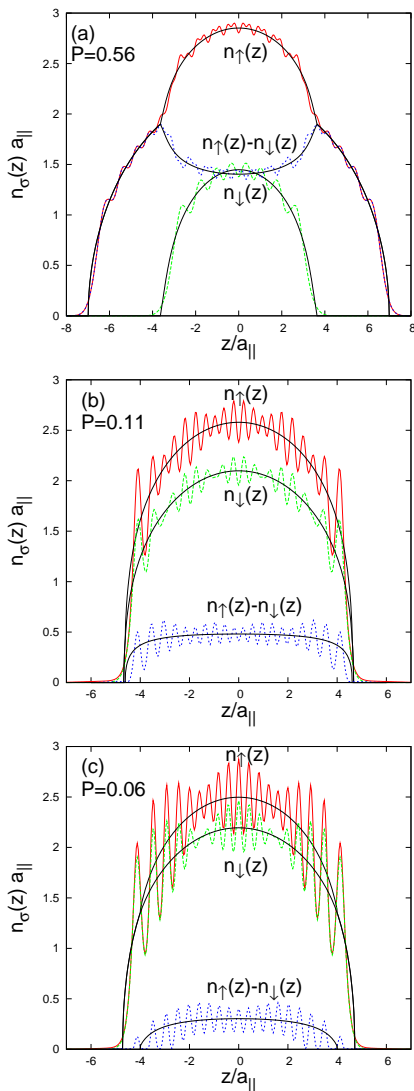


FIG. 5: (color online) The spin-up, spin-down and spin density profiles of fixed atom number $N = 36$ for $\eta = 1$. We show two different results based on the BALSDA (dotted lines) and the TFA (solid line between the oscillatory BALSDA results). (a) For $P = 0.56$, a two-shell structure is formed with a partially polarized FFLO-type superfluid of distinctive oscillatory character in the center of the trap and a fully polarized state at the edges. (b) For $P = 0.11$, a two-shell structure is formed with a partially polarized superfluid in the center of the trap and a fully paired superfluid state at the edges. (c) For $P = 0.06$, a smaller polarization gives larger BCS regime in the wings. In all the calculations, we show the TFA results give a good overall shape between the oscillating BALSDA ones.

But importantly, the TFA could not produce oscillation structure due to correlation effects in the quantum system.

V. CONCLUSIONS

In conclusion, we have presented two alternative methods to study the imbalanced two-component Fermi atomic gases of attractive interactions in Q1D harmonic traps. One is the spin-density-functional theory based on Bethe-ansatz solutions, which properly incorporates the Luther-Emery nature and the spin energy gap of the homogeneous system. Another is the TFA which takes a local density approximation for the noninteracting kinetic energy but including the exchange-correlation energy. We apply these two methods to the system of finite size trapped by the harmonic confinement. At weak coupling strength of any polarization or intermediate coupling of large polarization, a two-shell structure is obtained with a partially polarized pairs of FFLO-type state in the core and a fully polarized fermions in the wings. At intermediate coupling regime of small polarization, a two-shell structure is formed of partially polarized pairs of FFLO-type state in the bulk and a fully paired BCS state at the edges which is different from the 3D case. In the current experimental set-up, imbalanced interacting Fermi gases can be induced by a radio-frequency sweep in the optical lattice system, and in the on-going experiments, the two-shell structure described here should be observable in the system of thousands of Q1D tubes formed in the quasi-two-dimensional optical lattices with each of the tube containing up to 100 atoms measured by absorption imaging techniques, while the direct test of FFLO states remains as a challenge to experimental community [31].

It would be of interest to develop the present scheme to study dynamical phenomena in these strongly correlated gases using time-dependent DFT and/or current-DFT, instead of resorting to the inhomogeneous Tomonaga-Luttinger liquid model. From a more formal DFT viewpoint, a functional better than the one presented in Eq. (14) is desirable and necessary to deal with the strong coupling regime.

Acknowledgments

G. Xianlong was supported by NSF of China under Grant NO. 10704066. We would like to thank Hui Hu, Marco Polini and Saeed Abedinpour for many useful discussions.

-
- [1] H. Moritz, T. Stöferle, K. Günter, M. Köhl, and T. Esslinger, *Phys. Rev. Lett.* **94**, 210401 (2005).
- [2] B. Paredes, A. Widera, V. Murg, O. Mandel, S. Filling, I. Cirac, G. V. Shlyapnikov, T. W. Honsch, and I. Bloch, *Nature (London)* **429**, 277 (2004); T. Kinoshita, T. Wenger, and D. S. Weiss, *Science* **305**, 1125 (2004).
- [3] L. Tonks, *Phys. Rev.* **50**, 955 (1936); M. Girardeau, *J. Math. Phys.* **1**, 516 (1960); M. Girardeau, *Phys. Rev.* **139**, B500 (1965).
- [4] M. Olshanii, *Phys. Rev. Lett.* **81**, 938 (1998); T. Bergeman, M. G. Moore, and M. Olshanii, *ibid.* **91**, 163201 (2003).
- [5] O. Juillet, F. Gulminelli, and Ph. Chomaz, *Phys. Rev. Lett.* **92**, 160401 (2004).
- [6] M. D. Girardeau and A. Minguzzi, *Phys. Rev. Lett.* **96**, 080404 (2006); A. Minguzzi and M. D. Girardeau, *Phys. Rev. A* **73**, 063614 (2006).
- [7] G. Xianlong and W. Wonneberger, *Phys. Rev. A* **65**, 033610 (2002) and *J. Phys. B* **37**, 2363 (2004).
- [8] A. Recati, P. O. Fedichev, W. Zwerger, and P. Zoller, *Phys. Rev. Lett.* **90**, 020401 (2003) and *J. Opt. B* **5**, S55 (2003).
- [9] L. Kecke, H. Grabert, and W. Häusler, *Phys. Rev. Lett.* **94**, 176802 (2005).
- [10] G. E. Astrakharchik, D. Blume, S. Giorgini, and L. P. Pitaevskii, *Phys. Rev. Lett.* **93**, 050402 (2004); G. E. Astrakharchik, *Phys. Rev. A* **72**, 063620 (2005).
- [11] G. Xianlong, M. Polini, R. Asgari, and M. P. Tosi, *Phys. Rev. A* **73**, 033609 (2006).
- [12] M. W. Zwierlein, A. Schirotzek, C. H. Schunck, and W. Ketterle, *Science* **311**, 492 (2006).
- [13] G. B. Partridge, W. Li, R. I. Kamar, Y. Liao, and R. G. Hulet, *Science* **311**, 503 (2006).
- [14] G. Orso, *Phys. Rev. Lett.* **98**, 070402 (2007).
- [15] H. Hu, X.-J. Liu, and P. D. Drummond, *Phys. Rev. Lett.* **98**, 070403 (2007).
- [16] M. M. Parish, S. K. Baur, E. J. Mueller, and D. A. Huse, arXiv:0709.1120v1.
- [17] G. G. Batrouni, M. H. Huntley, V. G. Rousseau, and R. T. Scalettar, arXiv:0710.1353v1.
- [18] A. E. Feiguin and F. Heidrich-Meisner, arXiv:0707.4172v3.
- [19] M. Tezuka and M. Ueda, arXiv:0708.0894v1.
- [20] M. Gaudin, *Phys. Lett. A* **24A**, 55 (1967); C. N. Yang, *Phys. Rev. Lett.* **19**, 1312 (1967).
- [21] S. H. Abedinpour, M. Polini, G. Xianlong, and M. P. Tosi, *Phys. Rev. A* **75**, 015602 (2007).
- [22] R. J. Magyar and K. Burke, *Phys. Rev. A* **70**, 032508 (2004).
- [23] R. J. Magyar, arXiv:0708.3265v1
- [24] M. T. Batchelor, M. Bortz, X. W. Guan, and N. Oelkers, *Journal of Physics Conference Series* **42**, 5 (2006).
- [25] J. B. Bahder and F. Woynarovich, *Phys. Rev. B* **33**, 2114 (1986); K. Lee and P. Schlottmann, *Phys. Rev. B* **40**, 9104 (1989); C. Yang, A. N. Kocharian, and Y. L. Chiang, *J. Phys.: Condens. Matter* **12**, 7433 (2000).
- [26] R. M. Dreizler and E. K. U. Gross, *Density Functional Theory* (Springer, Berlin, 1990); G. F. Giuliani and G. Vignale, *Quantum Theory of the Electron Liquid* (Cambridge University Press, Cambridge, 2005).
- [27] A. Luther and V.J. Emery, *Phys. Rev. Lett.* **33**, 589 (1974); V. J. Emery, in *Highly Conducting One-Dimensional Solids*, edited by J.T. Devreese, R. P. Evrard, and V. E. van Doren (Plenum, New York, 1979).
- [28] F. D. M. Haldane, *J. Phys. C* **14**, 2585 (1981); H. J. Schulz, G. Cuniberti, and P. Pieri, in *Field Theories for Low-Dimensional Condensed Matter Systems*, edited by G. Morandi *et al.* (Springer, Berlin, 2000); T. Giamarchi, *Quantum Physics in One Dimension* (Clarendon Press, Oxford, 2004).
- [29] X.-J. Liu, H. Hu, and P. D. Drummond, *Phys. Rev. A* **76**, 043605 (2007).
- [30] Y. Shin, M. W. Zwierlein, C. H. Schunck, A. Schirotzek, and W. Ketterle, *Phys. Rev. Lett.* **97**, 030401 (2006); G. B. Partridge, W. Li, Y. A. Liao, R. G. Hulet, M. Haque, and H. T. C. Stoof, *Phys. Rev. Lett.* **97**, 190407 (2006).
- [31] Y. Chen, Z. D. Wang, F. C. Zhang, and C. S. Ting, arXiv:0710.5484v1.